Design and Validation of a Polycentric Hybrid Knee Prosthesis with Electromagnet-Controlled Mode Transition

Xu Wang[1], Haohua Xiu[1], Yao Zhang[1], Wei Liang[1], Wei Chen[1], Guowu Wei[2], *Member, IEEE*, Lei Ren[1,3], *Member, IEEE* and Luquan Ren[1]

Abstract—**A hybrid knee prosthesis is proposed in this paper, which consists of a polycentric structure in passive mode for low-torque activities and a single-axis structure in active mode for high-torque activities. A novel mode transition mechanism controls self-holding electromagnets for switching modes between the four-bar linkage and single-axis structure. Compared with the conventional single-axis hybrid knee, the four-bar polycentric mechanism with varying instantaneous center of rotation (ICR) can enhance the geometric stability and increase the toe clearance in passive mode. For active mode, we developed a custom embedded electric system, employed torque control for stance and position control for swing. The results of bench tests indicated that the bandwidth of the controller was suitable for locomotion. The clinical test of level-ground walking without sudden buckling and stumble was validated by three subjects. Regarding climbing stairs, a typical high-torque activity in daily locomotion, all subjects reach the maximum knee torque around 0.95 Nm/kg comparable to the able-bodied.**

Index Terms—**Prosthetics and exoskeletons, actuation and joint mechanisms**

I. INTRODUCTION

In our world, some people lose their lower limbs and must deal with a variety of mobility issues. With the prevalence of vascular disease, estimates indicate that the incidence of amputation and stroke will increase rapidly in the coming decades [1]. The knee prosthesis is committed to enhancing daily movement as a rehabilitation assistant device for transfemoral amputees.

Passive knee prostheses occupy the market due to their

lightweight and durable structure [2]. Most commercial mechanical passive knees use a hydraulic or pneumatic cylinder to conduct a smooth swing and stable stance [3]. In addition, microprocessor-controlled passive knee prostheses like the Ottobock® C-leg and Ossur® Rheo Knee can intelligently adjust the damping in a gait, allowing them to perform well in a wide range of users and environments [4, 5]. However, the passive knees are unable to support activities that need the injection of power (e.g., sit-to-stand and stair ascent).

To extend the range of activities, the fully active knee prosthesis is proposed. The active knee can help users go upstairs or stand up from a seat by providing energy injection and restoring the symmetry of movement. The only commercially available active knee is the Ossur® POWER KNEE™, which has a weight of 3.2 kg [6] and a height of 270 mm, and aims to restore muscular function. However, due to its higher price, shorter lifespan, and larger weight than the widely used commercial passive knees, just a few people wear the POWER KNEE™. The knee with power injection has more functions at the expense of an increase in device weight relative to passive devices. The tradeoff between weight and more functions is a challenge for the design of knee prostheses with power injection. In addition, some research groups are working on developing a variety of active knees. MIT proposed a MC-RFSEA knee to mimic the biological kinetic and kinematic function of a healthy knee [7]. With enhancing the effectiveness and clinical viability of the fully active knee, the University of Utah introduced an actively variable transmission to reduce the weight of the prosthesis, which still can provide enough torque and speed to assist locomotion [8]. The University of Michigan has developed a low-impedance knee with a high-torque actuator and low-reduction transmission [9] as well as an open-source knee for other researchers developing control strategies on a unified hardware platform [10]. To enhance the robustness of swing for reducing the likelihood of falls, the Vanderbilt University presented a stance-control, swing-assist (SCSA) knee prosthesis [11], and then described stair ambulation control and validated its performance with three subjects [12]. Although the active knee has more functions than the passive knee, its reliability of control, function/weight tradeoff, and short lifespan are challenging before it can be widely used for amputees.

Furthermore, the University of Utah has developed a

lightweight hybrid knee [6, 13]. For different activities, the hybrid knee can switch between passive and active modes, combining the advantages of a mechanical passive knee and a fully active knee to perform a wide range of activities. However, the Utah hybrid knee utilizes a single-axis structure, but the geometric stability and toe clearance are insufficient in passive mode. The challenge of passive mode focuses on the ability to keep a safe stance and conduct a natural swing, which mainly depend on the structure design and the configuration of the damper-spring system, respectively. As for active mode, the transmission system should meet the torque requirements of daily locomotion for amputees.

In this paper, we present a polycentric hybrid knee prosthesis with an electromagnet-controlled mode transition structure (PHKP-EC), innovatively introducing the four-bar polycentric structure into a hybrid knee with decoupled passive-active modes. The four-bar linkage for the spring-damper passive mode is paired with a single-axis structure for the motor-driven active mode in the PHKP-EC. In passive mode, the four-bar polycentric structure has the advantages of providing more geometric stability in stance and larger toe clearance in swing than the single-axis hybrid knees. The enhanced stability will reduce the likelihoods of falls at heel strike, the most critical period of stance for knee security, and the greater toe clearance will decrease the probability of stumble in swing.

Our PHKP-EC switches to passive mode for more frequent tasks requiring low torque in daily life, such as level-ground walking. On the other hand, the PHKP-EC switches to active mode for activities demanding high torque, such as going upstairs/upslope and sit-to-stand. This hybrid structure with both passive and active modes can conduct more activities and improve the reliability when active control fails. In our new mode transition mechanism, self-holding electromagnets are installed in the telescopic slide rails, switching between the passive mode's four-bar linkage and the active mode's single-axis structure, which responses fast.

II. MECHATRONIC DESIGN

A. Overview

To meet the requirements of amputees' daily activities, we mainly focus on the design of size, weight, range of motion (ROM), and maximum torque of the knee prosthesis. The CAD model in Fig. 1 shows an overview of the PHKP-EC mechatronic design. After iterative design, the build height of the PHKP-EC is 290 mm, and the total weight of the knee, including the control system and battery, is 3.3 kg. In passive mode, the ROM of the knee is 0 to 130°, and in active mode, it is 0 to 90°. [14] demonstrates that the typical stair ascent requires high torque, which acts as a representative task to verify the active mode. The PHKP-EC is designed to achieve a maximum torque of 95 Nm in active mode.

B. Passive mode

In a healthy knee joint, the instantaneous center of rotation (ICR) varies in response to the knee angle [15]. In our design for passive mode, the PHKP-EC turns into a four-bar linkage structure, which mimics the trajectory of healthy people's ICR

and provides more geometric stability and larger toe clearance than a single-axis knee. Low-torque activities are frequently performed in the passive mode, such as level-ground walking [14]. Moreover, some special activities (such as sitting in a cramped space/car) also can be easily supported in passive mode with its large ROM. The four-bar linkage is represented by the chain ABCD, as seen in Fig. 2(a). The instantaneous center of rotation (ICR) is located at the intersection of the directions of links AD and BC. The ICR of the PHKP-EC during flexion and extension is depicted by the green dotted line.
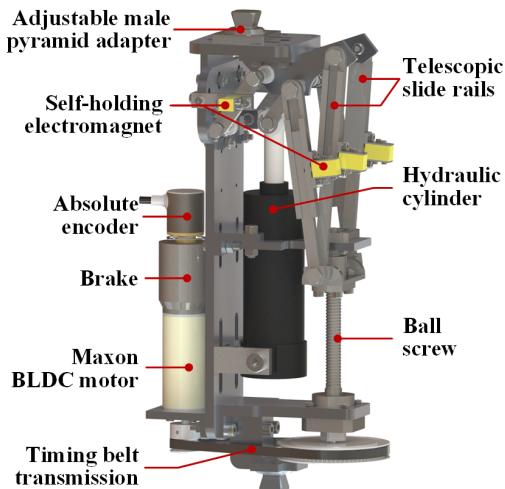

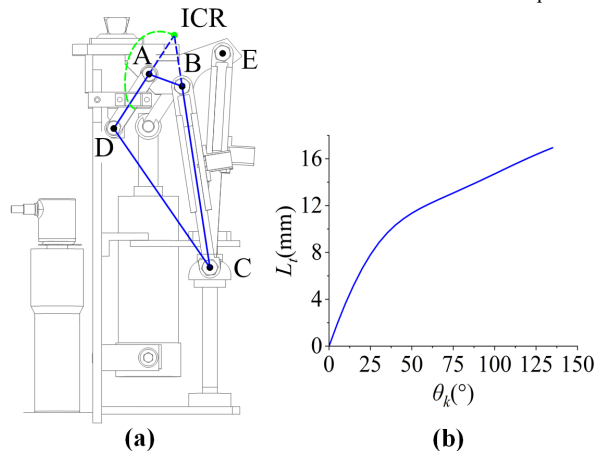Fig. 1 The CAD model of PHKP-EC with callouts of the main components.

Fig. 2 (a) The four-bar linkage (ABCD) for passive mode. The green dotted line represents the trajectory of the ICR. (b) The length of travel of hydraulic cylinder as a function of knee angle ($L_t(\theta_k)$).

During the stance phase, we expect the prosthesis to have a high level of stability to avoid unexpected buckling. In the swing phase, the effortless initial flexion and smooth movement are dedicated to performing a natural gait. Consequently, as shown in Fig. 3, we iteratively design the four-bar linkage to get enough stability. The user can voluntarily control the knee in passive mode using their hip.

At heel strike, the user voluntarily controls the ICR to be posterior to the load line with little hip effort in full extension of the knee, seeing in Fig. 3(a). Because the ICR is inside the stability zone while the foot is flat on the ground in Fig. 3(b), the user can flex voluntarily while remaining stable with hip movement. In Fig. 3(c), the ICR is located prior to the load line

during push off, allowing for easy entry into swing. The actual capacity of voluntarily controlling an unexpected flexion into a stable status, especially at heel strike, is largely determined by the physical capabilities of user. After a period of training, an experienced amputee can naturally control the stability of knee.

For comparison with single-axis hybrid knees such as [13, 16], we hypothetically regard joint A (orange point in Fig. 3(a), biomechanical axis of knee crossing hip-ankle line) as the single rotation center of a single-axis hybrid knee. At heel strike, the most important period of stance for knee security, the ICR is posterior to the joint A so that the PHKP-EC can be forced to provide more full extension moment to avoid unexpected buckling, providing more geometric stability. As shown in Fig. 3(a), the distance from ICR in our PHKP-EC to load line is longer than that from joint A in single-axis design to load line, which leads to more knee extension moment about the ICR than joint A. More knee extension moment at heel strike will decrease the chance of unexpected buckling, which may lead to a stumble. When walking on uneven ground or perturbations occurring, the user can voluntarily control the polycentric knee stability with more knee extension moment and less hip efforts than a single-axis design. In Fig. 3(b), the stability zone is defined by superimposing figures 3(a) and 3(c), which still maintains the features of stability at heel strike and ease of knee flexion at push off. The PHKP-EC is designed with the initial ICR located above the common knee joint A and well inside the stability zone.
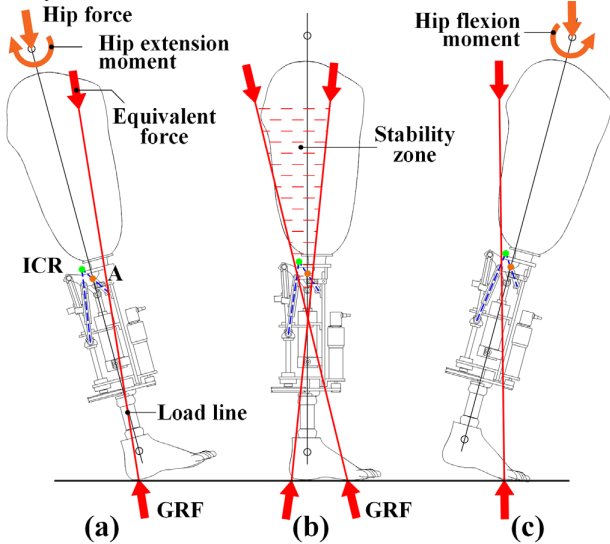

Fig. 3 Stability diagrams for passive mode. We hypothetically replace the force and moment acting on the hip joint with the equivalent force acting along the load line, and the magnitude of that equivalent force is equal to the ground reaction force (GRF). (a) At heel strike with the knee angle of 0°, the ICR (green point) is located behind the load line. The knee can avoid unexpected buckling with little hip extension moment due to its strong geometric stability. (b) In middle stance, the ICR is in the stability zone, which superimposes Fig. 3(a) and 3(c) for controlling the knee stability with the available hip moment. (c) At push off, the ICR moves prior to the load line, the knee can flex easily.

Furthermore, the PHKP-EC also provides more toe clearance to reduce the chance of stumble than the single-axis hybrid knee. In level-ground walking, healthy people's minimum toe clearance happens at a hip angle of 49° and a knee angle of 23° [17]. Referring to the above values, the simulation in

Solidworks® shows that the minimum toe clearance of the PHKP-EC is 13 mm, while a single-axis design offers a minimum toe clearance of 11 mm. So, the four-bar PHKP-EC produces a 2 mm (18%) greater than the single-axis knee. Regarding the condition that healthy people reach their maximum knee angle of 66.7° (hip angle of 10.7° [14]) during walking, the toe clearance of the PHKP-EC is 8 mm (11%) larger than that of a single-axis hybrid knee.

We assembled a damper-spring system with a hydraulic cylinder (Blatchford, Endolite 932281) in passive mode to provide a smooth swing and compliant interaction with ground. It is worth to say that the hydraulic cylinder, as described in [13, 16], has little influence on the active mode. The resistive passive torque provided by damper-spring system can be calculated by the virtual work principle, as shown in (1). $T_p(\theta_k)$ is the resistive passive torque with respect to the knee angle θ_k, and F_t is the force produced by the hydraulic cylinder depending on its length of travel L_t and deformation velocity $\dot{L}_t$.

$$T_p(\theta_k)\dot{\theta}_k = F_t(L_t, \dot{L}_t)\dot{L}_t \tag{1}$$

After simulation in Solidworks®, the length of linear travel $L_t(\theta_k)$ can be computed as a function of knee angle θ_k as shown in Fig. 2(b). So (1) can be described as,

$$T_p(\theta_k) = F_t(L_t(\theta_k), \frac{\partial L_t(\theta_k)}{\partial \theta_k}\dot{\theta}_k)\frac{\partial L_t(\theta_k)}{\partial \theta_k} \tag{2}$$

C. Active mode

The PHKP-EC is configured as a single-axis mechanism in active mode. After the iterative design with avoiding interference and ensuring compactness, we optimally govern the transmission ratio and moment arm to be large enough at the first 55° of knee angle in stance, where covers the torque requirements for most torque-demanding activities. As indicated in Fig. 4, joint A is the fixed center of rotation of the knee. Moreover, in active mode, the length of link EC is fixed by the self-holding electromagnet locking the rails, and the link AD is immobilized by the electromagnet, as discussed in Section II-D. The motor drives the active actuation system by injecting energy, allowing it to achieve high-torque tasks like reciprocal stair climbing. In Fig. 4(a), the L_m denotes the length of moment arm which is simply the distance between joint A and the link EC acting on joint A. The value of moment arm presents in Fig. 4(b), indicating that it is sufficient to meet the torque requirement in stance at the knee angle of first 55°.

As shown in fig 4(a), the origin of the coordinates locates at the revolute joint A, and the coordinate of the ball-screw nut is represented by C (a, λ). θ_1 is the angle between link AE and the positive x-axis. The lower part of the knee, is assumed to be immobile in the following kinematics study, whereas the top part of the knee rotates around the joint A. So, the knee angle θ_k and the displacement of the nut s can be derived as

$$\theta_k = \theta_{1\_initial} - \theta_1 \tag{3}$$

$$s = \lambda_0 - \lambda \tag{4}$$

$$s = \frac{p_t}{p_s} \cdot \frac{1}{n_b} \cdot ph \tag{5}$$

This article has been accepted for publication in IEEE Robotics and Automation Letters. This is the author's version which has not been fully edited and content may change prior to final publication. Citation information: DOI 10.1109/LRA.2022.3193462

4   IEEE ROBOTICS AND AUTOMATION LETTERS. PREPRINT VERSION. ACCEPTED JULY 2022

where the $\theta_{1\_initial}$ and λ_0 are initial values of θ_1 and λ in full extension of the knee, respectively. p_t represents the total pulses of motor absolute encoder, p_s represents the single turn pulses, n_b is the teeth ratio of the timing belt transmission, and ph is the lead of the ball screw.
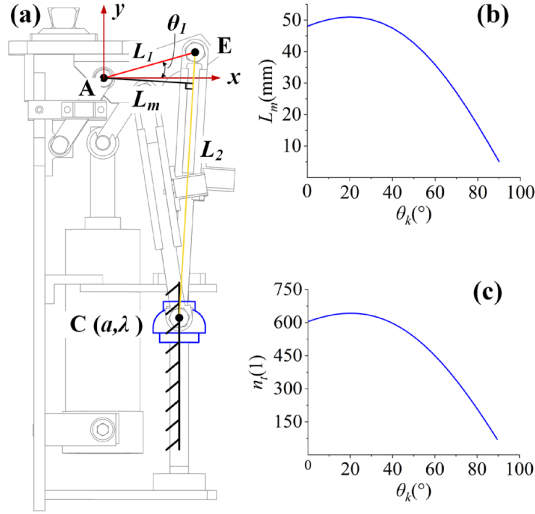

Fig. 4 (a) The kinematics of the active mode. (b) The magnitude of the moment arm with respect to the knee angle. (c) The transmission ratio from motor to knee joint with respect to the knee angle.

The coordinates of joint E are $(L_1\cos\theta_1, L_1\sin\theta_1)$. The length of link EC can be expressed as

$$(L_1\cos\theta_1 - a)^2 + (L_1\sin\theta_1 - \lambda)^2 = L_2^2 \qquad (6)$$

and rewritten as

$$\lambda^2 - 2L_1\sin\theta_1\lambda + L_1^2 - L_2^2 + a^2 - 2aL_1\cos\theta_1 = 0 \qquad (7)$$

In (7), one can obtain the θ_1 from the λ, a is constant. Then (7) can be simplified as

$$M\sin\theta_1 + N\cos\theta_1 + Q = 0 \qquad (8)$$

where, $M = -2L_1$, $N = -2L_1 a$, $Q = L_1^2 - L_2^2 + a^2 + \lambda^2$

The angle θ_1 depends on the nut's position λ, which can be expressed as

$$\theta_1 = 2\arctan\frac{M - \sqrt{M^2 + N^2 - Q^2}}{N - Q} \qquad (9)$$

The transmission ratio from the ball screw to knee joint n is

$$n = \frac{ds}{d\theta_k} = \frac{d(\lambda_0 - \lambda)}{d(\theta_{1\_initial} - \theta_1)} = \frac{d\lambda}{d\theta_1} = \frac{L_1\lambda\cos\theta_1 - aL_1\sin\theta_1}{\lambda - L_1\sin\theta_1} \qquad (10)$$

The transmission ratio from motor to the knee joint n_t can be calculated, and its value with respect to the knee angle is shown in Fig. 4(c).

$$n_t = n \cdot \frac{2\pi}{ph} \cdot n_b \qquad (11)$$

D. Mode transition

A new mode transition structure based on telescopic slide rails controlled by self-holding electromagnets is proposed in this section. As shown in Fig. 5(a), telescopic slide rails comprise an inner rail and an outer rail. The off-the-shelf self-holding electromagnet (dimensions of the shell: 8 mm*10.3 mm*16.3 mm, diameter of iron shaft: 4 mm) is fixed

on the outer rail and the output shaft plugs into the telescopic slide rails. The output shaft will extend if the self-holding electromagnet is powered with a forward voltage. The output shaft will then jam the outer rail and the inner rail to bear the load of ambulation, causing the telescopic slide rails locked. Conversely, if a backward voltage is applied to the self-holding electromagnet, the output shaft retracts and unlocks the telescopic slide rails, allowing the outer and inner rails to slide relatively. The self-holding electromagnet can hold on to the locked/unlocked state without continues power and keep stable during walking. In Fig. 5(b), the switching between passive mode and active mode depends on the state of the self-holding electromagnet, which extends or retracts its iron output shaft to lock or unlock the telescopic slide rails, respectively.
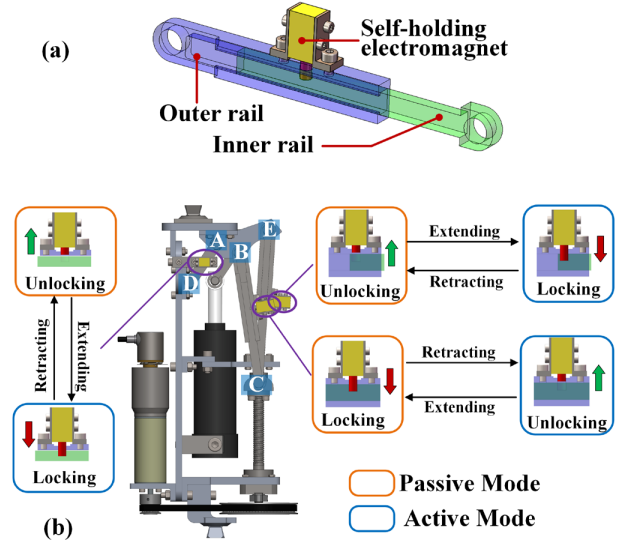

Fig. 5 (a) Mode transition mechanism. The telescopic slide rails consist of an inner rail and an outer rail. The self-holding electromagnet is mounted on the outer rail. (b) The switching process between active mode and passive mode. The state of each self-holding electromagnet in passive mode is shown in the orange box, and that in active mode is shown in the blue box.
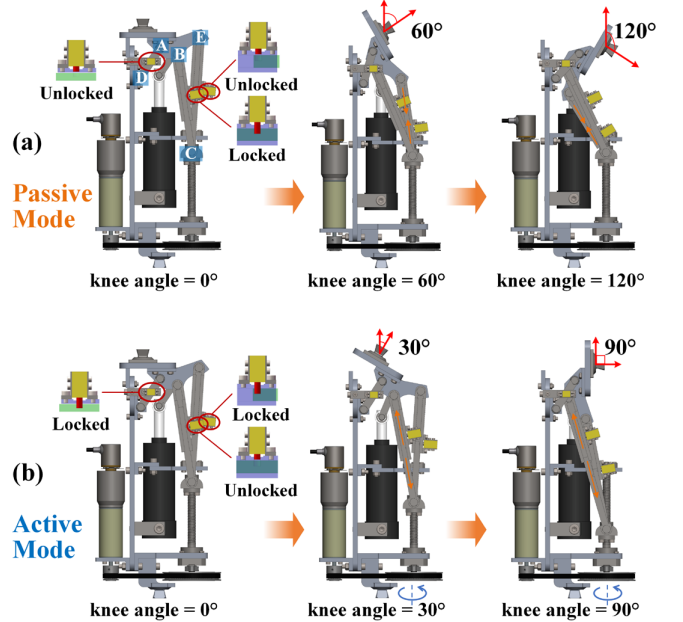

Fig. 6 (a) The knee switches to four-bar passive mode and rotates to 60° and 120°, the brake immobilizing the screw. (b) The knee switches to single-axis active mode and rotates to 30° and 90°.

The mode transition occurs at knee angle of 0° and the user stops locomotion in stance, meanwhile the telescopic slide rails and the ball-screw nut are driven at the recorded absolute position. During switching, there is no movement in the multi-bar mechanism, and the mode transition can be stably completed. As shown in Fig. 6(a), the telescopic slide rails EC is unlocked since the electromagnet's output shaft retracts, allowing the inner and outer rails to slide relatively. Meanwhile, the telescopic slide rails BC is locked as the output shaft extends, and the output shaft does not plug into the link AD for moving freely. Therefore, the PHKP-EC switches to the polycentric passive mode. Furthermore, the brake immobilizes the motor's output shaft so that the ball-screw nut can be fixed, avoiding up-and-down movements.

As shown in Fig. 6(b), in active mode, the rotation of the knee is driven by the motor. The telescopic slide rails EC is locked as its output shaft of the electromagnet extends, while the telescopic slide rails BC is unlocked as the output shaft retracts, and the link AD is fixed.

Unlike the fully active knee prosthesis, the hybrid knee can switch to passive mode when the battery runs out or the control fails during active mode. Hence, even with no power injection for high-torque activities (e.g., going upstairs in a step-over-step pattern), the knee can still flex in passive mode and ensure the user completes the task exactly like a typical passive knee (e.g., going upstairs in a step-by-step pattern). Consequently, the mode transition mechanism has the potential to improve prosthesis reliability.

E. Actuation system

Firstly, we chose a high-power density motor (Maxon, EC-4pole 30 mm 200 W) to generate enough torque. A brake (Maxon) is mounted on the end of the motor to ensure that the ball screw and nut in passive mode are not disturbed during walking. Furthermore, because the absolute position of nut should be recorded for mode transition, the PHKP-EC configures an absolute encoder (Scancon, 2RMHF-SSI). A ball screw (lead 2 mm, pitch diameter 10 mm) and the motor are connected by a timing belt transmission (72:18 teeth ratio).

III. CONTROL SYSTEM

A. Electrical hardware

We designed a compact embedded system in Fig. 7(a), 95 mm *83 mm in size, to provide sensing and control for the PHKP-EC. The custom embedded system consists of a 32-bit microchip (STM32F429ZIT6) as the joint controller unit (JCU). The six-axis inertial measurement unit (IMU) is employed for sensing the motion attitude used for intention recognition (recognizing different activities) in future work, communicating with the JCU via the IIC bus, and the analog-to-digital converter (ADC) can collect the voltage of the force sensing resistor (FSR) for monitoring whether the foot contacts the ground. The microSD card located on the motherboard is used for data storage. The JCU communicates with the motor driver via the high-speed CAN bus. The serial port on the board, which complies with the RS232 standard, can connect to the computer and collect data in real time.

As shown in Fig. 7(b), a 24-V li-ion battery powers the EPOS4 motor driver and the custom embedded system. The self-holding electromagnet, FSR and onboard module all get power from the 24-V supply, which is regulated to 7 V, 5 V and 3.3 V, respectively. In addition, the brake connected to the input/output (I/O) port can be switched off to lock the motor's output shaft. For mode transition, an absolute encoder connected to the driver and complying with the SSI standard records the absolute position of the motor.
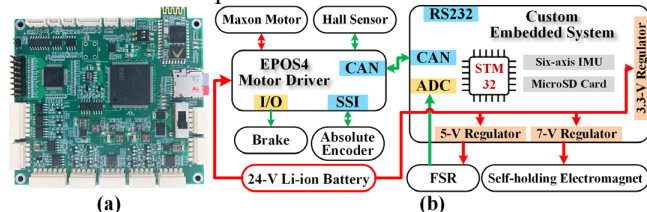

Fig. 7 (a) Top view of the custom embedded system. (b) Block diagram of electrical hardware. The motor driver connects with the embedded system via the CAN bus.

B. Middle-level Control

For active mode, we designed the typical control strategy for reciprocal stair ascent, which requires the high torque in daily activities. The generalized controller of prosthesis is hierarchically divided into three levels [18]: high-level for intention recognition, middle-level for intent-to-state conversion, and low-level for motor control. We will discuss high-level control in future work.
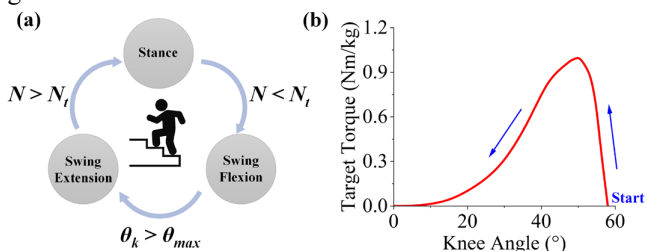

Fig. 8 (a) Phase transition criteria for middle-level control. (b) Torque-angle curve for stance phase control.

The finite-state machine (FSM) is widely used in middle-level controllers [9, 12, 13] for powered lower limb prostheses. Under varying transition criteria, the FSM divides a gait into several phases. In the PHKP-EC, a gait for going upstairs is divided into three phases: stance, swing flexion, and swing extension in Fig. 8(a). In stance phase, the foot is considered to touch the ground when the force N detected by the FSR is greater than the threshold N_t. Once the foot leaves the ground, the prosthesis enters the swing flexion phase, sensing the N less than the N_t. Next, the knee joint flexes beyond the maximum angle θ_{max}, allowing the prosthetic foot to clear the step, and then enters the swing extension phase to reach an appropriate angle for pre-landing. When the foot contacts the step again, the prosthesis completes one gait cycle and moves on to the next.

C. Low-level Control

The low-level control is configured to ensure a stable stance and a smooth swing. Some researchers conduct the impendence control with an open-loop torque controller, such as the

Vanderbilt Generation 3 knee [19], the MIT CSEA knee [20], and the Low-impendence knee [9]. However, the impendence control should devote a significant amount of time to fine-tuning the parameters in the controller. Furthermore, the University of Utah imposed a torque–angle relationship for the controller [13], which mimics the relationship between normalized torque and knee angle of healthy people, implementing the torque accurately and visually. For stair ascent, referring to the dataset in [14], the low-level controller of the PHKP-EC looks up the torque-angle table in stance with torque control. The torque-angle curve reference is shown in Fig. 8(b). The prosthesis flexes to about 58° and then starts to step on the staircase. The prosthesis extends to near 0° in late stance with power injection. Noting that, according to the feedback from the subjects in the real test, the torque controller configures the desired maximum torque of 0.98 Nm/kg at the knee angle around 51°, which is slightly higher than the able-bodied data (0.84 Nm/kg) in [14].

In swing phase, the JCU sends target position signals to the motor driver. With the feedback of the absolute encoder, the motor rotates to the target position in position mode. The driver can precisely implement position control around the motor.

IV. BENCH TESTS

A. Methods

Before the subject tests, we conducted the bench tests to evaluate the performance of position and torque controllers for active mode. The step response test was used to evaluate the dynamic response of the closed-loop position controller. As demonstrated in Fig. 9(a), the top pyramid of PHKP-EC was connected to the testing jig and can flex freely. Starting at 0°, we set each desired position to 5°, 10°, and 15°, respectively. The mean and standard deviations of the measured knee angles were obtained in post-processing after each step was repeated five times. The mean rise times were used for calculating the -3 dB bandwidth of the system,

$$BW = \frac{0.35}{t_r} \tag{12}$$

where the BW and t_r represent the mean values of the bandwidth and the rise time, respectively.

In the torque step response test in Fig. 10(a), the actual torque was obtained by multiplying the measured reaction force by the moment arm about joint A. The top of the knee was mounted on the testing jig at the knee angle of 0°, and the bottom of knee was against a load cell (Sunrise Instruments, M3564F) that measured the reaction force at a sampling frequency of 400 Hz. The desired torque of each step was set to 15 Nm, 25 Nm, and 35 Nm, respectively. We also repeated each step five times. The -3 dB bandwidth was calculated using the same method as the position step response.

B. Results

Fig. 9(b) depicts the results of position step response. The mean rise times of trajectories were 46 ms, 85 ms, and 120 ms, corresponding to the desired knee angles of 5°, 10° and 15°, respectively. By using (12), the estimated -3 dB bandwidths for

the desired positions of 5°, 10°, and 15° were 7.6 Hz, 4.1 Hz, and 2.9 Hz, respectively.

In Fig. 10(b), the mean and standard deviation of the measured torque were used to evaluate the performance of torque controller. For steps of 15 Nm, 25 Nm, and 35 Nm, the mean rise times were 117 ms, 112 ms, and 120 ms, respectively. The corresponding estimated -3 dB bandwidths were 3.0 Hz, 3.1 Hz, and 2.9 Hz. The results of the bench tests revealed that the bandwidth of the system was suitable for amputee's locomotion, since the knee position and torque data for healthy people were characterized by frequencies at or below 1~2 Hz [19, 21].
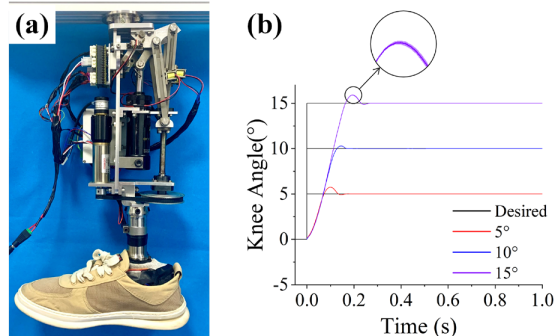

Fig. 9 Bench test for the position control. (a) Setup for position step response test. (b) The mean and standard deviation of position step response. The partial enlargement highlights the standard deviation.
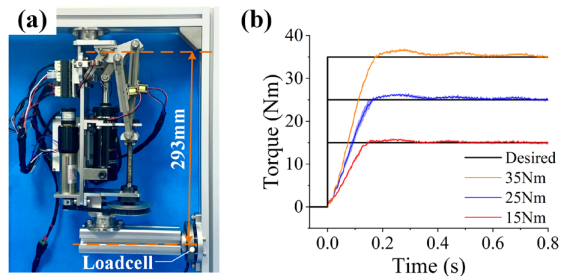

Fig. 10 Bench test for the torque control. (a) Setup for torque step response test. The load cell measuring the reaction force is mounted on the testing jig and the moment arm about joint A is 293mm. (b) The mean and standard deviation of torque step response.

V. CLINICAL VALIDATIONS

To evaluate the performance of the PHKP-EC in practical use, clinical validations should be undertaken after the bench tests. We measured the knee angle and torque in both active and passive modes and compared them with able-bodied individuals. Three participants (subject 1: male, 32 years old, 168 cm, 65 kg; subject 2: male, 32 years old, 166 cm, 75 kg; subject 3: male, 31 years old, 181 cm, 80 kg) were invited to complete all the tests. All subject experiments were approved by the Ethics Committee of the Second Hospital of Jilin University (Log # 2021072).

A. Passive mode test

For the gait analysis of the passive mode of the PHKP-EC, we used a six-camera motion capture system (Vicon, UK) to conduct the walking test (Fig. 11(a)). In addition, three force plates embedded in the ground were used to collect data of the GRF. Before the test, a certified prosthetist adjusted the height

of the pylon, aligned the prosthesis, and configured the damping level of the hydraulic cylinder for each subject.

After about 20 minutes of training, we started recording the data, and each subject walked five times from the first to the last force plate at a self-selected speed. Referring to [22], the position of the markers attached to the lower limbs of the subjects with their associated GRF data were measured for computing the knee angle and torque.
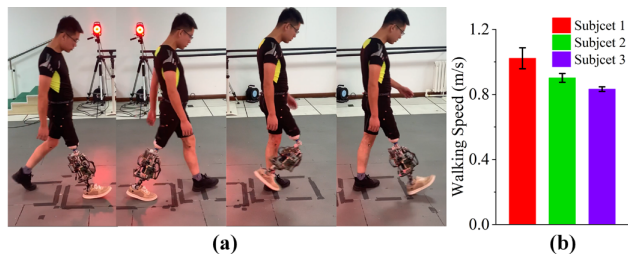

Fig. 11 (a) Level-ground walking in passive mode. (b) The walking speed.
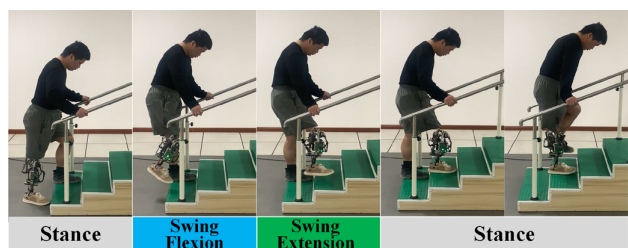

Fig. 12 Stair ascent test in active mode.

B. Active mode test

To evaluate the performance of the active mode of the PHKP-EC, the stair ascending in a step-over-step pattern was carried out. We began recording the data collected by the embedded system via serial port after about half an hour of training. The standard training staircase was recommended by the China Rehabilitation Medical Association, with a uniform height of 12.5 cm and a uniform width of 65 cm. Each subject proceeded upstairs five times at a self-selected speed, and five strides were performed, as illustrated in Fig. 12. The knee angle was computed in (3) and the knee torque was estimated by multiplying the motor torque by the transmission ratio.

C. Results

Fig. 13(a) shows the knee angle and normalized torque of three subjects during the level-ground walking test in passive mode. The similar trend of the trajectories revealed that the PHKP-EC can assist the amputees in regaining their walking ability. Unlike the able-bodied subjects, the prosthesis did not flex during the early stance (stride: 0% - 20%), since its geometric stability results in a full extension in passive mode, which provides more safety to avoid unexpected buckling. The measured maximum knee angles (79°, 81° and 70°) were higher than the healthy one (68°) as the subjects must tread on large-gap force plates. The maximum knee torque of the prosthesis is lower than the healthy data as there is no power injection in passive mode. The other joints of the body must output considerably more power to compensate for the lack of torque in the knee joint for locomotion. The Fig. 11(b) of

walking speed shows that the subject 1 walks fast and the subject 3 walks slow. So, subject 3 has a lower peak knee angle and torque than others.
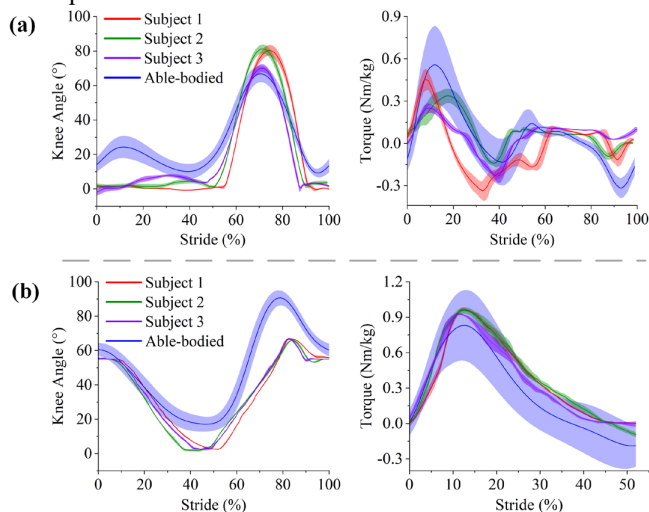

Fig. 13 Results of (a) level-ground walking test in passive mode and (b) stair ascent test in active mode. Trajectories of measured mean knee angle and knee torque of three subjects were compared with the dataset [14] of 22 able-bodied subjects. The shaded areas present the standard deviations. The knee angle in (b) shows small standard deviation because it was obtained in (3) based on encoder data, which was precisely regulated by position control in motor driver.

The prosthesis was switched to active mode for stair ascending. As shown in Fig. 13(b), in swing, all subjects reached the maximum angle later than the able-bodied, and the maximum angle was lower, because the maximum angle in position controller was set lower based on the height of staircase. We computed the knee torque at first 52% of the stride (stance phase) where the prosthesis employs torque control. The maximum knee torque of subject 1 was 0.96 Nm/kg (standard deviation: 0.013) at 12% of the stride, which is 0.13 Nm/kg (15%) larger than the healthy people (0.84 Nm/kg at 13% of the stride). Subject 2 achieved maximum torque of 0.95 Nm/kg (standard deviation: 0.026) at 12% of the stride which is 0.12 Nm/kg (14%) higher than the healthy people. Subject 3 reached the maximum torque of 0.93 Nm/kg (standard deviation: 0.01) at 11% of the stride, which is faster than subjects 1 and 2. Compared with the other two subjects, subject 1 presents a shorter duration of full extension stance (around the knee angle of 0°) during going upstairs, due to the strong strength of his residual limb.

VI. Discussion

A. Polycentric structure

The single-axis mechanism (often employed in passive microprocessor-controlled knee, fully powered knee, and hybrid knee) has the advantages of small size, lightweight, and strong capacity of flexion stance due to its simple structure. On the contrary, the polycentric structure normally owns the large weight/size and poor capacity for stance flexion, but can enhance the geometric stability and increase the toe clearance.

The four-bar polycentric structure is innovatively employed in our hybrid knee for passive mode. Due to the longer distance from ICR to load line, our polycentric structure has more extension moment than a single-axis hybrid knee, and the

geometric stability is provided for avoiding unexpected buckling at heel strike in passive mode. Unlike the common single-axis knee that can easily conduct knee flexion in stance, our polycentric passive mode implements geometric stability instead, which gives more safety. In swing, the minimum toe clearance in our polycentric structure increases 18% more than that in a single-axis design, reducing the chance of stumble.

Our polycentric structure has above more functions at the expense of an increase in weight/size relative to the single-axis mechanism. We will carry out structural optimization to reduce the weight/size in future work.

B. Mode transition

A new mode transition mechanism is presented for this polycentric hybrid knee, which contains the telescopic slide rails controlled by the self-holding electromagnet. The mode transition can switch between passive mode for low-torque activities and active mode for high-torque activities, which performs a large range of activities and has the potential to improve prosthesis reliability.

The telescopic slide rails are well employed in this multi-bar polycentric structure to avoid the mechanical interference between the active mode and passive mode. As for the small and cheap self-holding electromagnet, the duration required for the locking/unlocking operation of the self-holding electromagnet is around 0.3s, which can fast control the switching between active mode and passive mode. Compared with the typical Utah hybrid knee [13], whose mode transition consists of an actively variable transmission with a motor and leadscrew controlling the crank length, our mode transition design has a short duration (0.3 s vs. 0.6 s). Meanwhile, the Utah hybrid knee must use another motor controller for mode transition except the main controller for the primary motor, but our design can be directly controlled by the embedded system, which is a simple and efficient approach.

VII. CONCLUSION

We proposed a polycentric hybrid knee prosthesis with an electromagnet-controlled mode transition mechanism. In passive mode, the four-bar polycentric structure promotes the geometric stability in stance and toe clearance in swing than the single-axis hybrid knees. The mode transition system is designed with a new electromagnet-controlled telescopic slide rails to switch between the active mode and passive mode in this multi-bar mechanism. The control system was developed, including the electrical hardware, the torque control for stance, and position control for swing. Furthermore, bench tests and clinical validations were conducted. The subjects were requested to walk under the motion capture system and proceed upstairs reciprocally. The results of bench tests revealed that the bandwidth can satisfy the needs of amputees and the results of clinical tests show similar trajectories of knee angle and torque to that of the healthy body.

Future work will focus on the high-level control (intention recognition) and the reduction of weight. Moreover, more subjects should be considered for the clinical validation.

REFERENCES

[1] D. J. Villarreal and R. D. Gregg, "Controlling a Powered Transfemoral Prosthetic Leg Using a Unified Phase Variable," in *Wearable Robotics*: Elsevier, 2020.

[2] M. A. Price, P. Beckerle, and F. C. Sup, "Design Optimization in Lower Limb Prostheses: A Review," *IEEE Transactions on Neural Systems and Rehabilitation Engineering,* vol. 27, no. 8, pp. 1574-1588, 2019.

[3] T. M. Köhler, M. Bellmann, and S. Blumentritt, "Polycentric Exoprosthetic Knee Joints – Extent of Shortening during Swing Phase," *Canadian Prosthetics & Orthotics Journal,* vol. 3, no. 1, 2020.

[4] M. R. Meier, A. H. Hansen, S. A. Gard, and A. K. McFadyen, "Obstacle course: users' maneuverability and movement efficiency when using Otto Bock C-Leg, Otto Bock 3R60, and CaTech SNS prosthetic knee joints," *Journal of Rehabilitation Research & Development* vol. 49, no. 4, pp. 583-96, 2012.

[5] M. Bellmann, T. Schmalz, and S. Blumentritt, "Comparative Biomechanical Analysis of Current Microprocessor-Controlled Prosthetic Knee Joints," *Archives of Physical Medicine and Rehabilitation,* vol. 91, no. 4, pp. 644-652, 2010.

[6] T. Lenzi, M. Cempini, L. Hargrove, and T. Kuiken, "Hybrid actuation systems for lightweight transfemoral prostheses," in *2017 Design of Medical Devices Conference*, Minneapolis, Minnesota, USA, 2017.

[7] M. E. Carney, T. Shu, R. Stolyarov, J.-F. Duval, and H. M. Herr, "Design and Preliminary Results of a Reaction Force Series Elastic Actuator for Bionic Knee and Ankle Prostheses," *IEEE Transactions on Medical Robotics and Bionics,* vol. 3, no. 3, pp. 542-553, 2021.

[8] M. Tran, L. Gabert, M. Cempini, and T. Lenzi, "A Lightweight, Efficient Fully Powered Knee Prosthesis With Actively Variable Transmission," *IEEE Robotics Automation Letters,* vol. 4, no. 2, pp. 1186-1193, 2019.

[9] T. Elery, S. Rezazadeh, C. Nesler, and R. D. Gregg, "Design and Validation of a Powered Knee–Ankle Prosthesis With High-Torque, Low-Impedance Actuators," *IEEE Transactions on Robotics,* vol. 36, no. 6, pp. 1649 - 1668, 2020.

[10] A. F. Azocar, L. M. Mooney, J. F. Duval, A. M. Simon, L. J. Hargrove, and E. J. Rouse, "Design and clinical implementation of an open-source bionic leg," *Nature Biomedical Engineering,* vol. 4, no. 10, pp. 941-953, 2020.

[11] J. T. Lee, H. L. Bartlett, and M. Goldfarb, "Design of a Semi-Powered Stance-Control Swing-Assist Transfemoral Prosthesis," *IEEE/ASME Transactions on Mechatronics,* vol. 25, no. 1, pp. 175 - 184, 2019.

[12] J. T. Lee and M. Goldfarb, "Effect of a swing-assist knee prosthesis on stair ambulation," *IEEE Transactions on Neural Systems and Rehabilitation Engineering,* vol. 29, pp. 2046-2054, 2021.

[13] T. Lenzi, M. Cempini, L. Hargrove, and T. Kuiken, "Design, development, and testing of a lightweight hybrid robotic knee prosthesis," *The International Journal of Robotics Research,* vol. 37, no. 8, pp. 953-976, 2018.

[14] J. Camargo, A. Ramanathan, W. Flanagan, and A. Young, "A comprehensive, open-source dataset of lower limb biomechanics in multiple conditions of stairs, ramps, and level-ground ambulation and transitions," *Journal of Biomechanics,* vol. 119, 2021.

[15] M. Olinski, A. Gronowicz, and M. Ceccarelli, "Development and characterisation of a controllable adjustable knee joint mechanism," *Mechanism and Machine Theory,* vol. 155, 2021.

[16] T. Lenzi, J. Sensinger, J. Lipsey, L. Hargrove, and T. Kuiken, "Design and preliminary testing of the RIC hybrid knee prosthesis," presented at the 2015 37th Annual International Conference of the IEEE Engineering in Medicine and Biology Society (EMBC), Italy, 2015.

[17] D. A. Winter, "Foot trajectory in human gait: a precise and multifactorial motor control task," *Physical Therapy,* vol. 72, 1992.

[18] M. R. Tucker *et al.*, "Control strategies for active lower extremity prosthetics and orthotics: a review," *Journal of Neuroengineering and Rehabilitation,* vol. 12, no. 1, p. 1, 2015.

[19] B. E. Lawson, J. Mitchell, D. Truex, A. Shultz, E. Ledoux, and M. Goldfarb, "A robotic leg prosthesis: Design, control, and implementation," *IEEE Robotics Automation Magazine,* vol. 21, no. 4, pp. 70-81, 2014.

[20] E. J. Rouse, L. M. Mooney, and H. M. Herr, "Clutchable series-elastic actuator: Implications for prosthetic knee design," *The International Journal of Robotics Research,* vol. 33, no. 13, pp. 1611-1625, 2014.

[21] D. A. Winter, *Biomechanics and motor control of human movement*. John Wiley & Sons, 2009.

[22] D. G. E. Robertson, G. E. Caldwell, J. Hamill, G. Kamen, and S. Whittlesey, *Research methods in biomechanics (Second Edition)*. Human kinetics, 2013.